ENVIRONMENTAL RESEARCH
LETTERS

LETTER

The impact of particulate pollution control on aerosol hygroscopicity and CCN activity in North China

Yuxiang Wang[1,4], Yuying Wang[1,2,4,*], Xiaorui Song[1], Yi Shang[1], Yunxiang Zhou[1], Xin Huang[1] and Zhanqing Li[3]

[1] Key Laboratory for Aerosol-Cloud Precipitation of China Meteorological Administration, School of Atmospheric Physics, Nanjing University of Information Science & Technology, Nanjing 210044, People's Republic of China
[2] State Key Laboratory of Remote Sensing Science, College of Global Change and Earth System Science, Beijing Normal University, Beijing 100875, People's Republic of China
[3] Earth System Science Interdisciplinary Center and Department of Atmospheric and Oceanic Science, University of Maryland, College Park, MD, United States of America
[4] These authors contributed equally.
[*] Author to whom any correspondence should be addressed.

E-mail: yuyingwang@nuist.edu.cn

Keywords: North China, CCN, aerosol hygroscopicity, activation ability

Supplementary material for this article is available online

OPEN ACCESS

RECEIVED
10 March 2023

REVISED
9 June 2023

ACCEPTED FOR PUBLICATION
15 June 2023

PUBLISHED
27 June 2023

Abstract

Air quality has greatly improved in China owing to the strict control policy enforced during the last decade. This study investigated the impact of particulate pollution control on aerosol hygroscopicity and cloud condensation nuclei (CCN) activity in North China based on several data sources. The mass concentration of particles with an aerodynamic diameter smaller than 2.5 μm ($PM_{2.5}$) decreased by one third from the summer of 2014 to the summer of 2020 in Xinzhou (XZ). The mass fractions of aerosol chemical components in $PM_{2.5}$ also clearly changed, showing an increase in hydrophilic inorganics and a decrease in hydrophobic organics and black carbon from 2014 to 2020. Measurements of the particle number size distribution in XZ indicate that the occurrence frequency of new particle formation (NPF) events decreased significantly from 2014 to 2020, leading to a reduction in the generation of daytime ultrafine particles. The weakened NPF and increasing influence of morning and evening peak emissions modified the diurnal variations of the number concentration of condensation nuclei (N_{CN}) and CCN (N_{CCN}). The aerosol activation ratio was always higher in the summer of 2014 than in the summer of 2020. These results demonstrate that particulate pollution control can decrease N_{CN} and N_{CCN} but enhance aerosol hygroscopicity and activation ability.

1. Introduction

Aerosols, solid and liquid mixtures suspended in the atmosphere, have highly uncertain physicochemical properties. At a certain water vapor supersaturation (*SS*), some aerosol particles can be activated as cloud condensation nuclei (CCN) to form cloud droplets. CCN activity depends on particle size, chemical components, and mixing state (Wu *et al* 2013; Zhang *et al* 2017a). Anthropogenic emissions have a strong influence on aerosol physicochemical properties.

With rapid economic development over the past decades, extensive production in China has led to severe air pollution (Chan and Yao 2008). Through industrialization and urbanization, different emission sources and aging processes make aerosol physicochemical properties complicated and highly variable. The occurrence and evolution of haze have a great impact on the aerosol mixing state and chemical composition, among others (Wang *et al* 2021). Fossil fuel energy, represented by coal burning, is the main source of air pollution and carbon emission in China (Jin *et al* 2016).

Since the 1980s, air quality in China had been worsened until the most recent decade when increasing attention and efforts have been devoted to tackle this problem. Early air pollution control measures have had a limited effect, and their implementation

has been slow. Until the 11th Five-Year Plan began in 2006, air pollution control measures began to roll out gradually (Jin *et al* 2016). Data analyses and numerical simulations using the China High Air Pollutants (CHAP) dataset indicate that the mass concentration of particles with an aerodynamic diameter smaller than 2.5 μm ($PM_{2.5}$) increased before 2007 and remained at a high level until 2013. Several large-scale haze pollution events broke out in China at the beginning of 2013, finally capturing people's attention (Wang *et al* 2014). Following these events, the government issued a strict control policy to address the air pollution problem. Until 2017, $PM_{2.5}$ in most areas of China had significantly decreased compared with 2013 (Zhang *et al* 2019). Compared with 2015, mass concentrations of $PM_{2.5}$ in major cities in China in 2020 had also decreased (Li *et al* 2022). The sharp reduction in gaseous precursors and particulate matter is bound to have had an impact on aerosol physicochemical properties.

Aerosol hygroscopicity and CCN activity represent the interactions of aerosols and water vapor under subsaturated and supersaturated water vapor conditions. Aerosol hygroscopicity plays an important role in aerosol optical properties, atmospheric visibility, and atmospheric radiative forcings (Lohmann and Feichter 2005). CCN activity is closely related to the formation of clouds and precipitation and has an important impact on global climate change (Li *et al* 2011). In recent years, many studies about aerosol hygroscopicity and CCN activity in China have been carried out (Wang *et al* 2001, Zhao *et al* 2019). However, few studies have focused on the change in aerosol hygroscopicity and CCN activity after the implementation of air pollution control measures. This study is based on two field campaigns carried out at the same sampling site (Xinzhou (XZ), Shanxi Province) in 2014 and 2020 to explore changes in aerosol hygroscopicity and CCN activity in North China. Findings presented here may be useful as references for future air pollution controls.

This paper is organized as follows. Section 2 introduces the sampling site, instruments, and methods of data analysis. Section 3 describes the effect of emission reductions in recent years and compares the differences in aerosol hygroscopicity and CCN activity between 2014 and 2020 in XZ. Section 4 summarizes the research results.

2. Sampling site, instruments, and data analysis methods

2.1. The sampling site and background

In the summers of 2014 and 2020, two field observation experiments studying atmosphere, aerosol, boundary layer, and cloud interactions were conducted in XZ (38.24° N, 112.43° E). This sampling site is located in the north-central part of Shanxi Province, bordering Hebei Province by the Taihang Mountains to the east, Inner Mongolia to the northwest, and Shanxi Province across the Yellow River to the west (figure S1). The meteorological data in XZ during measurement periods between 2014 and 2020 are compared in figures S2–S5 and table S1. They show that there was a little difference of weather background between two measurement periods. The cluster analysis of air mass backward trajectories shows that most air masses influencing the measurement site were from the local sources (figure S6). Air quality had a general improvement during the COVID-19 lockdown period in the early 2020 in China although several severe hazes occurred in northern China due to the unfavorable meteorological condition (He *et al* 2020, Le *et al* 2020). However, most lockdown measures ended in April, 2020. Our measurement period is in summer (July–August). Figure S7 show that the $PM_{2.5}$ mass concentrations in July–August between 2019 and 2020 is considerable, which implies that the measurement period in 2020 is weakly affected by the COVID-19.

2.2. Instruments

During the two experiments, the scanning mobility particle sizer (SMPS, TSI Inc.) and CCN counter (CCNc, DMT Inc.) were connected to measure size-resolved number concentrations of condensation nuclei (N_{CN}) and CCN (N_{CCN}), following the method known as the scanning mobility CCN analysis (Moore *et al* 2010). Figure S8 shows a schematic diagram of the SMPS-CCNc system. The dryer and impactor in this system were used for drying the sample and blocking large particles. The neutralizer and differential mobility analyzer were applied to neutralize electrostatic charges on aerosol particles and select quasi-monodisperse particles with specific diameters. The sample flow was split into two paths. One path flowed into the condensation particle counter to count N_{CN}, and the other flowed into the CCNc to count N_{CCN}. Finally, the size-resolved activation ratio (AR) (N_{CCN}/N_{CN}) was retrieved after applying the multiple charge correction. From 22 July to 26 August 2014, the SMPS-CCNc system measured particles with diameters ranging from 11 to 594 nm every 10 min, while from 11 July to 6 August 2020, the system measured particles with diameters ranging from 7 to 300 nm every 5 min. The supersaturation (SS) of CCNc were 0.07%, 0.1%, 0.2%, 0.4%, and 0.8% in 2014 and 0.2%, 0.4%, 0.6%, 0.8%, and 1% in 2020.

Two different models of aerosol chemical speciation monitor (ACSM) were used to measure the mass concentrations of non-refractory aerosol chemical components, including organics (Org), sulfate (SO_4^{2-}), nitrate (NO_3^-), ammonium (NH_4^+), and chloride (Cl^-) in particles with an aerodynamic diameter smaller than 1 μm and 2.5 μm (PM_1 and $PM_{2.5}$)

in 2014 and 2020, respectively. The ACSMs used in 2014 and 2020 were equipped with different lens systems, so their measured particle size ranges were different (Wang *et al* 2016, 2021). Sun *et al* (2012) and Zhang *et al* (2017b) provided detailed descriptions of the ACSM.

Refractory black carbon (BC) aerosols were measured by aethalometers (Model AE-31 in 2014 and Model AE-33 in 2020, Magee Scientific Corp.). The operating principles of AE-31 and AE-33 are similar. The mass concentration of optically absorbing aerosols (i.e. BC) is retrieved from the rate of change of the attenuation of light transmitted through the filter, which collects aerosol particles through a spot.

The CHAP dataset is a remote sensing dataset of near-surface air pollutants with wide spatiotemporal coverage, high resolution, and high precision (Wei *et al* 2020, 2021). Tracking Air Pollution (TAP) is another dataset constructing multi-scale, near real-time aerosol and gas concentrations (Geng *et al* 2021). This study used the CHAP and TAP datasets to investigate the spatial distribution of $PM_{2.5}$ and aerosol chemical composition trends from the summer (June, July and August) of 2014–2020.

2.3. Data analysis methods

As described in section 2.2, the size-resolved AR (N_{CCN}/N_{CN}) can be retrieved from measurements made by the SMPS-CCNc system. The CCN efficiency spectra can be fitted using a cumulative Gaussian distribution function (CDF; Rose *et al* 2008):

$$f_{N_{CCN}/N_{CN}} = a\left(1+\mathrm{erf}\left(\frac{D-D_a}{\sigma\sqrt{2}}\right)\right) \quad (1)$$

where $f_{N_{CCN}/N_{CN}}$ is the AR, erf is the error function, a is the half-of-maximum activated fraction (MAF), D_a is the midpoint activation diameter, and σ is the CDF standard deviation. Ideally, a of internally mixed aerosols is 0.5.

The hygroscopicity parameter (κ) is commonly used to represent aerosol hygroscopicity and activation ability (Petters and Kreidenweis 2007). Assuming that particles are internally mixed, the κ of multicomponent aerosols can be estimated using aerosol chemical component data based on the Zdanovskii–Stokes–Robinson mixing rule (Stokes and Robinson 1966):

$$\kappa = \sum_i \varepsilon_i \kappa_i \quad (2)$$

where ε_i and κ_i are the volume fraction and κ for the ith chemical component, respectively. The parameters of common chemical components can be found in table S2.

Because the ACSM only obtains real-time mass concentration data about inorganic ions, the following ion-pairing scheme was used to obtain data about inorganic salts (Gysel *et al* 2007):

$$\begin{aligned} n_{NH_4NO_3} &= n_{NO_3^-} \\ n_{H_2SO_4} &= \max\left(0, n_{SO_4^{2-}} - n_{NH_4^+} + n_{NO_3^-}\right) \\ n_{NH_4HSO_4} &= \min\left(2n_{SO_4^{2-}} - n_{NH_4^+} + n_{NO_3^-}, n_{NH_4^+} - n_{NO_3^-}\right) \\ n_{(NH_4)_2SO_4} &= \max\left(n_{NH_4^+} - n_{NO_3^-} - n_{SO_4^{2-}}, 0\right) \\ n_{HNO_3} &= 0 \end{aligned} \quad (3)$$

where n is the number of moles.

3. Results and discussion

3.1. A wide range of temporal and spatial variation characteristics

Figures 1(a) and (b) show the spatial distributions of mean $PM_{2.5}$ mass concentration from the CHAP dataset in the summers of 2014 and 2020. Over most land areas of China, $PM_{2.5}$ mass concentrations in the summer of 2020 were clearly lower than in the summer of 2014, especially in North China. This confirms the effectiveness of particulate pollution control in recent years. The mean mass concentration of $PM_{2.5}$ in XZ was 38.13 μg m^{-3} in the summer of 2014 and 25.9 μg m^{-3} in the summer of 2020, decreasing by about one third from 2014 to 2020. Figures 1(c) and (d) show summertime mean mass concentrations of $PM_{2.5}$ and mean mass fractions of inorganics (SO_4^{2-}, NO_3^-, and NH_4^+), Org, and BC in $PM_{2.5}$ in XZ from the TAP dataset from 2014 to 2020. Figure 1(c) shows that the mean mass concentration of $PM_{2.5}$ in XZ decreased by about one third over this period. The overall trend of $PM_{2.5}$ in the TAP dataset is consistent with that in the CHAP dataset. In addition, the TAP dataset shows that the mass fractions of Org and BC decreased, and the total mass fraction of inorganics increased from 2014 to 2020 (figure 1(d)). This indicates that the decrease in primary aerosols (most BC and some organics) was stronger than that of secondary aerosols (most inorganics and some organics) due to the particulate pollution control. This phenomenon is common in China, related to the sharp decrease in primary emissions caused by industrial upgrading (Zhang *et al* 2016). Changes in the mass fractions of aerosol chemical components are bound to affect aerosol hygroscopicity and activation ability (Wu *et al* 2013, Zhang *et al* 2017a).

3.2. Aerosol chemical composition and particle number size distribution (PNSD)

Figure 2 shows the mean mass fractions of aerosol chemical components and the time series of PNSD in XZ during the two experiments in the summers of 2014 and 2020. The mean mass concentration of PM_1 was 33.97 μg m^{-3} in 2014, and that of $PM_{2.5}$ was 26.82 μg m^{-3} in 2020. Due to the difference in ACSM

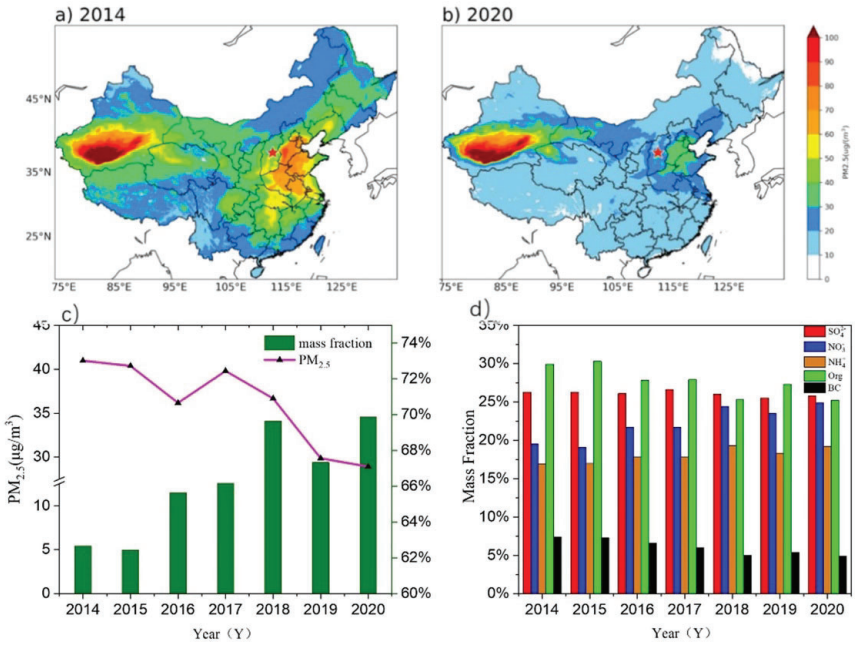

Figure 1. Spatial distributions of mean $PM_{2.5}$ mass concentration in the summers of (a) 2014 and (b) 2020 from the CHAP dataset. (c) Mean mass concentration of $PM_{2.5}$ and the total mass fraction of inorganics, and (d) mean mass fractions of aerosol chemical components in the summers from 2014 to 2020 from the TAP dataset.

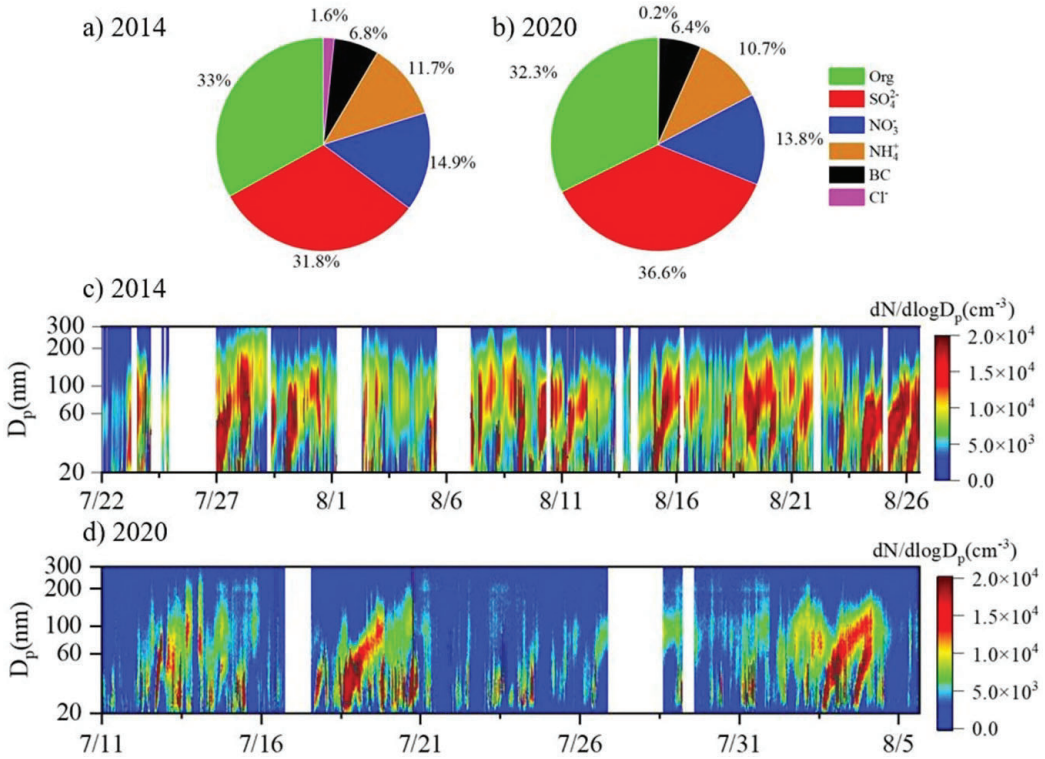

Figure 2. Mean mass fractions of aerosol chemical components (a) in PM_1 in the summer of 2014 and (b) in $PM_{2.5}$ in the summer of 2020. Time series of particle number size distributions in the summers of (c) 2014 and (d) 2020 during the two field experiments in XZ.

models, aerosol chemical components in PM_1 were measured in 2014, and aerosol chemical components in $PM_{2.5}$ were measured in 2020. Zhang *et al* (2018) and Chen *et al* (2020) indicated that PM_1 contributed mostly to $PM_{2.5}$ in North China. Figures 2(a) and (b) show that aerosol chemical components during the

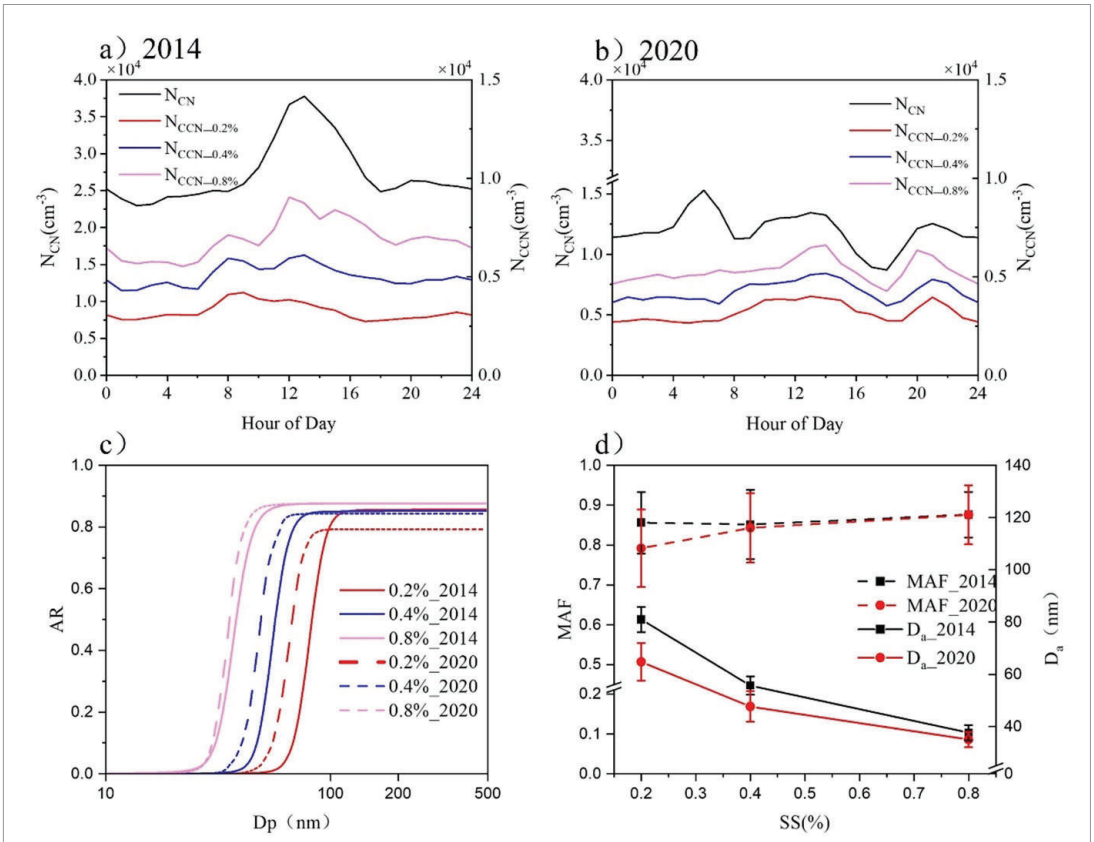

Figure 3. Diurnal variations of N_{CN} and N_{CCN} at different *SS* levels in (a) the summer of 2014 and (b) the summer of 2020 in XZ. (c) Mean size-resolved AR (AR curves) at different *SS* levels and (d) mean D_a and MAF with their standard deviations in the summers of 2014 and 2020.

measurement periods mainly consisted of Org and SO_4^{2-}, followed by NO_3^-, NH_4^+, and BC. From 2014 to 2020, the mass fraction of Org decreased slightly, and the mass fraction of SO_4^{2-} increased. Org and SO_4^{2-} were the dominant aerosol chemical components in 2014 and 2020, respectively. The total mass fraction of inorganics increased from 58.4% in 2014 to 61.1% in 2020. The weaker increase compared to that from the TAP dataset (figure 1(c)) is likely caused by the short-term nature of the measurements and the difference in aerosol chemical compositions between PM_1 and $PM_{2.5}$. Considering that the hygroscopicity of inorganics is much higher than Org, this implies that aerosol hygroscopicity should be enhanced due to particulate pollution control. The mean calculated κ using equation (2) was 0.38 in 2014 and 0.39 in 2020.

Figures 2(c) and (d) show that the PNSDs were distinct between the summers of 2014 and 2020. During the measurement period in the summer of 2014, new particle formation (NPF) events happened frequently (on 18 d out of 35 measurement days, about 51.5%). By contrast, NPF events occurred less often in the summer of 2020 (on 6 d out of 25 measurement days, about 24.0%). Mean diurnal variations of PNSD also show that the NPF event happened more frequently and strongly in summer 2014 than that in summer 2020 (figures S9 and S10). This suggests that the reduction in primary emissions including the emission reduction of gaseous precursors can have a big impact on the generation of ultrafine particles.

3.3. CCN number concentration and aerosol activation ability

To investigate aerosol hygroscopicity and activation ability in XZ, N_{CN} and N_{CCN} data at the same *SS* (0.2%, 0.4%, and 0.8%) observed during the two experiments were analyzed. N_{CN} and N_{CCN} were always higher in 2014 than in 2020. The diurnal variations of N_{CN} and N_{CCN} in the summer of 2014 show a unimodal or quasi-unimodal pattern, peaking near noon (figure 3(a)). With the increase in N_{CN} during the day, N_{CCN} also increased, especially at high *SS* levels (0.4% and 0.8%). This indicates that the frequent NPF events that occurred in the summer of 2014 had a large impact on N_{CN} and N_{CCN}. Unlike 2014, the diurnal variation of N_{CN} in the summer of 2020 has three peaks, one in the early morning and the others after the morning and after evening rush hours (figure 3(b)). The two N_{CN} peaks in the early morning and after the evening rush hours are likely related to the descending boundary layer height and nocturnal emissions. Figure S9 indicates that these factors

have different impact on N_{CN} in different modes. The increase in N_{CN} during the early morning had a weak influence on N_{CCN}, likely because the sizes of the increasing number of particles were small (figure S10(b)). The increase in N_{CCN} in the daytime in the summer of 2020 was weaker than that in the summer of 2014. This implies that the impact of photochemical reactions on N_{CN} and N_{CCN} weakened due to particulate pollution control.

Figure 3(c) shows the mean size-resolved AR (the AR curve, fitted by equation (1)) for different *SS* levels in the summers of 2014 and 2020. In general, AR increased as *SS* increased. The D_a and MAF, with their standard deviations for the AR curves, are shown in figure 3(d). D_a was always less than 100 nm for all SS levels considered. The D_a in the summer of 2020 was always smaller than that in the summer of 2014, with a larger standard deviation. According to the κ-Köhler theory (Petters and Kreidenweis 2007), a smaller D_a at the same *SS* means stronger aerosol hygroscopicity and activation ability. All this illustrates that particulate pollution control can decrease N_{CN} and N_{CCN} but enhance aerosol hygroscopicity and activation ability. MAF at low SS (0.2%) in the summer of 2020 was lower than that in the summer of 2014 and similar at high SS (0.4% and 0.8%). The standard deviation of MAF in 2020 was slightly higher than that in 2014. The smaller MAF in 2020 is likely related to the weakened NPF events.

4. Conclusions

In the last decade, air pollution has been greatly reduced in China due to the implementation of a strict control policy. This study first investigates the impact of particulate pollution control on aerosol hygroscopicity and CCN activity in North China based on measurements from two field experiments carried out in XZ in the summers of 2014 and 2020 and two other datasets, i.e. the CHAP and TAP datasets.

The CHAP and TAP datasets suggest that the mass concentration of particles with an aerodynamic diameter smaller than 2.5 μm ($PM_{2.5}$) decreased by one third from the summer of 2014 to the summer of 2020, demonstrating the effectiveness of particulate pollution control in this region. The TAP dataset also indicates that the decrease in primary aerosols (most black carbon and some organics) was stronger than that of secondary aerosols (most inorganics and some organics) due to the particulate pollution control. This led to a significant increase in the total mass fraction of inorganics in $PM_{2.5}$ from 2014 to 2020, changing aerosol hygroscopicity and activity.

The short-term field measurements made in XZ also suggest an increase in the total mass fraction of inorganics from 2014 to 2020. The PNSD illustrates that the occurrence frequency of NPF events in the summer of 2020 was much lower than that in the summer of 2014 (24.0% vs. 51.5%). Ultrafine particles increased and grew during the day in the summer of 2014, seen to a weaker degree in the summer of 2020. This illustrates that the secondary formation of ultrafine particles was inhibited due to particulate pollution control.

The analysis of the number concentrations of N_{CN} and CCN (N_{CCN}) suggests that the diurnal variations of N_{CN} and N_{CCN} changed from 2014 to 2020. The diurnal variations of N_{CN} and N_{CCN} show unimodal or quasi-unimodal patterns in the summer of 2014 and multimodal patterns in the summer of 2020 due to the weakened NPF and the enhanced influence of morning and evening peak emissions. The size-resolved AR further suggests that particulate pollution control can decrease N_{CN} and N_{CCN} but enhance aerosol hygroscopicity and activation ability.

Data availability statements

The data that support the findings of this study are openly available at the following URL/DOI: https://pan.baidu.com/s/1q1pwJ9Bns0YyCwsXMo7Tdg?pwd=42bf.

Acknowledgments

This work was funded by the National Natural Science Foundation of China (NSFC) research project (Grant Nos. 42005067, 42030606, and 92044303). We thank all participants in the field campaign for their tireless work and cooperation.

Conflict of interest

The authors declare no competing interests.

ORCID iD

Yuying Wang https://orcid.org/0000-0001-9762-8563

References

Chan C K and Yao X 2008 Air pollution in mega cities in China *Atmos. Environ.* **42** 1–42

Chen C, Zhang H, Li H, Wu N and Zhang Q 2020 Chemical characteristics and source apportionment of ambient $PM_{1.0}$ and $PM_{2.5}$ in a polluted city in North China plain *Atmos. Environ.* **242** 117867

Geng G *et al* 2021 Tracking air pollution in China: near real-time $PM_{2.5}$ retrievals from multisource data fusion *Environ. Sci. Technol.* **55** 12106–15

Gysel M, Crosier J, Topping D, Whitehead J D, Bower K N, Cubison M J, Williams P I, Flynn M J, McFiggans G B and Coe H 2007 Closure study between chemical composition and hygroscopic growth of aerosol particles during TORCH2 *Atmos. Chem. Phys.* **7** 6131–44

He G, Pan Y and Tanaka T 2020 The short-term impacts of COVID-19 lockdown on urban air pollution in China *Nat. Sustain.* **3** 1005–11

Jin Y, Andersson H and Zhang S 2016 Air pollution control policies in China: a retrospective and prospects *Int. J. Environ. Res. Public Health* **13** 1219

Le T, Wang Y, Liu L, Yang J, Yung Y L, Li G and Seinfeld J H 2020 Unexpected air pollution with marked emission reductions during the COVID-19 outbreak in China *Science* **369** 702–6

Li Y, Zhang Z and Xing Y 2022 Long-term change analysis of $PM_{2.5}$ and ozone pollution in China's most polluted region during 2015–2020 *Atmosphere* **13** 104

Li Z, Niu F, Fan J, Liu Y, Rosenfeld D and Ding Y 2011 Long-term impacts of aerosols on the vertical development of clouds and precipitation *Nat. Geosci.* **4** 888–94

Lohmann U and Feichter J 2005 Global indirect aerosol effects: a review *Atmos. Chem. Phys.* **5** 715–37

Moore R H, Nenes A and Medina J 2010 Scanning mobility CCN analysis—a method for fast measurements of size-resolved CCN distributions and activation kinetics *Aerosol Sci. Technol.* **44** 861–71

Petters M D and Kreidenweis S M 2007 A single parameter representation of hygroscopic growth and cloud condensation nucleus activity *Atmos. Chem. Phys.* **7** 1961–71

Rose D, Gunthe S S, Mikhailov E, Frank G P, Dusek U, Andreae M O and Pöschl U 2008 Calibration and measurement uncertainties of a continuous-flow cloud condensation nuclei counter (DMT-CCNC): CCN activation of ammonium sulfate and sodium chloride aerosol particles in theory and experiment *Atmos. Chem. Phys.* **8** 1153–79

Stokes R H and Robinson R A 1966 Interactions in aqueous nonelectrolyte solutions. I. Solute-solvent equilibria *J. Phys. Chem.* **70** 2126–31

Sun Y, Wang Z, Dong H, Yang T, Li J, Pan X, Chen P and Jayne J T 2012 Characterization of summer organic and inorganic aerosols in Beijing, China with an Aerosol Chemical Speciation Monitor *Atmos. Environ.* **51** 250–9

Wang M, Zhang R and Pu Y 2001 Recent researches on aerosol in China *Adv. Atmos. Sci.* **18** 576–86

Wang Q *et al* 2016 Characterization of submicron aerosols at a suburban site in central China *Atmos. Environ.* **131** 115–23

Wang Y S, Yao L, Wang L L, Liu Z, Ji D, Tang G, Zhang J, Sun Y, Hu B and Xin J 2014 Mechanism for the formation of the January 2013 heavy haze pollution episode over central and eastern China *Sci. China Earth Sci.* **57** 14–25

Wang Y *et al* 2021 Enhancement of secondary aerosol formation by reduced anthropogenic emissions during Spring Festival 2019 and enlightenment for regional $PM_{2.5}$ control in Beijing *Atmos. Chem. Phys.* **21** 915–26

Wei J *et al* 2020 Improved 1-km resolution $PM_{2.5}$ estimates across China using enhanced space-time extremely randomized trees *Atmos. Chem. Phys.* **20** 3273–89

Wei J, Li Z, Lyapustin A, Sun L, Peng Y, Xue W, Su T and Cribb M 2021 Reconstructing 1-km-resolution high-quality $PM_{2.5}$ data records from 2000 to 2018 in China: spatiotemporal variations and policy implications *Remote Sens. Environ.* **252** 112136

Wu J Z *et al* 2013 Relating particle hygroscopicity and CCN activity to chemical composition during the HCCT-2010 field campaign *Atmos. Chem. Phys.* **13** 7983–96

Zhang F *et al* 2016 Impacts of organic aerosols and its oxidation level on CCN activity from measurement at a suburban site in China *Atmos. Chem. Phys.* **16** 5413–25

Zhang F, Wang Y, Peng J Ren J, Collins D, Zhang R and Li Z 2017a Uncertainty in predicting CCN activity of aged and primary aerosols *J. Geophys. Res.: Atmos.* **122** 711–23

Zhang Q *et al* 2019 Drivers of improved $PM_{2.5}$ air quality in China from 2013 to 2017 *Proc. Natl Acad. Sci.* **116** 24463–9

Zhang Y, Lang J, Cheng S, Li S, Zhou Y, Chen D, Zhang H and Wang H 2018 Chemical composition and sources of PM and PM in Beijing in autumn *Sci. Total Environ.* **630** 72–82

Zhang Y, Tang L, Croteau P L, Favez O, Sun Y, Canagaratna M R and Worsnop D R 2017b Field characterization of the $PM_{2.5}$ Aerosol Chemical Speciation Monitor: insights into the composition, sources, and processes of fine particles in Eastern China *Atmos. Chem. Phys.* **17** 1–52

Zhao C, Yu Y, Tao J and Zhao G 2019 Recent progress of aerosol light-scattering enhancement factor studies in China *Adv. Atmos. Sci.* **36** 1015–26